

1     **U-Pb dating and Sm-Nd isotopic analysis of granitic rocks**  
2     **from the Tiris Complex: New constraints on key events in the**  
3     **evolution of the Reguibat Shield, Mauritania**

4  
5     **D. I. Schofield<sup>1</sup>, M. S. A. Horstwood<sup>2</sup>, P. E. J. Pitfield<sup>3</sup>, M. Gillespie<sup>4</sup>, F.**  
6     **Darbyshire<sup>2</sup>, E. A. O'Connor<sup>3</sup> & T. B. Abdouloye<sup>5</sup>**

7  
8     <sup>1</sup>*British Geological Survey, Columbus House, Cardiff, CF15 7NE, UK*  
9     *(e-mail: dis@bgs.ac.uk)*

10    <sup>2</sup>*NERC Isotope Geoscience Laboratory, Kingsley Dunham Centre, Nottingham NG12*  
11    *5GG, UK*

12    <sup>3</sup>*British Geological Survey, Keyworth, Nottingham, NG12 5GG, UK*

13    <sup>4</sup>*British Geological Survey, Murchison House, West Mains Road, Edinburgh,*  
14    *Scotland, EH9 3LA, UK*

15    <sup>5</sup>*DMG, Ministère des Mines et de l'Industrie, Nouakchott, RIM.*

16  
17  
18    **Abstract:** The Reguibat Shield of N Mauritania and W Algeria represents the  
19    northern exposure of the West African Craton. As with its counterpart in equatorial  
20    West Africa, the Leo Shield, it comprises a western Archaean Domain and an eastern  
21    Palaeoproterozoic Domain. Much of the southern part of the Archaean Domain is  
22    underlain by the Tasiast-Tijirit Terrane and Amsaga Complex which, along with the  
23    Ghallaman Complex in the northeast, preserve a history of Mesoarchaeon crustal  
24    growth, reworking and terrane assembly. This study presents new U-Pb and Sm-Nd  
25    data from the Tiris Complex, a granite-migmatite-supracrustal belt, that intervenes  
26    between these units and the Palaeoproterozoic Domain to the northeast.

27    New U-Pb geochronology indicates that the main intrusive events, broadly  
28    associated with formation of dome-shaped structures, occurred at around 2.95 to 2.87  
29    Ga and 2.69 to 2.65 Ga. This study also recognises younger regional metamorphism  
30    and intrusion of syn-tectonic granites located within major shear zones at around 2.56  
31    to 2.48 Ga. Sm-Nd depleted mantle model ages indicate that magmatism involved  
32    recycling of crustal source components older than at least 3.25 Ga in age. Comparison  
33    with other Archaean units in the Reguibat Shield and in the Leo Shield illustrate the

34 importance of deformation and tectonism of a regional greenstone-sedimentary  
35 province prior to around 3.00 Ga as well as subsequent magmatic episodes broadly  
36 equivalent in age to those in the Tiris Complex.

37

38

## 39 **1. Introduction**

40

41 The Reguibat Shield of N Mauritania and W Algeria comprises an uplifted  
42 area of Precambrian rocks that has been stable since about 1.70 Ga. It forms the  
43 northern area of exposure of the West African Craton, the southern being the Leo  
44 Shield of equatorial West Africa (Fig. 1). Both shield areas comprise a western  
45 domain of mainly Archaean metamorphic and granitic rocks and an eastern domain of  
46 largely Palaeoproterozoic granitic and volcano-sedimentary rocks (Bessoles, 1977;  
47 Dillon & Sougy, 1974). In Mauritania, these crustal domains were juxtaposed during  
48 the, *c.* 2.10-2.00 Ga, Eburnean Orogeny (Schofield et al., 2006).

49 This paper is based on recent 1: 200,000 scale reconnaissance geological  
50 surveying combined with geochronological and whole rock isotopic studies from the  
51 Tiris Complex (O'Connor et al., 2005), a granitoid-migmatite-supracrustal belt  
52 exposed near the NE margin of the Archaean Domain (Fig. 2). The main aim is to  
53 provide an account of the geological features, provide new geochronological  
54 framework for this otherwise poorly reported region and consider their bearing on the  
55 overall evolution of the shield and West African Craton as a whole.

56

57

## 58 **2. Geological setting**

59 Rocci et al. (1991) proposed simplified 'lithostratigraphic domains' for the  
60 Archaean part of the Reguibat Shield: the Tasiast-Lebzenia domain in its southwest  
61 part; the Amsaga-Tiris-Ouassat domain in its central part; and the Ghallaman domain  
62 in its eastern part. The former has recently been reclassified as the Tasiast - Tijirit  
63 Terrane (Pitfield et al., 2005). The Amsaga-Tiris-Ouassat domain is herein treated as  
64 separate lithostratigraphic entities named Tiris and Amsaga complexes. The discreet  
65 assemblage of gneisses and intrusive igneous rocks of the Ghallaman domain is herein  
66 referred to as a Complex for consistency (Fig. 2). The Ouassat Complex has recently  
67 been shown to comprise accreted parts of the eastern Palaeoproterozoic Domain

68 (Schofield et al., 2006). The term “Choum-rag el Abiod Terrane” was introduced by  
69 Key et al. (2008) for the eastern part of the Archaean Domain and is largely  
70 synonymous with the Amsaga Complex. However, as the northward extension of this  
71 unit was not defined as part of that study, we have reverted to the older nomenclature.

72

### 73 2.1. *Tasiast – Tijirit Terrane*

74

75 The Tasiast - Tijirit Terrane comprises tonalitic and granitic gneisses  
76 interleaved with amphibolitic units interpreted as remnants of older greenstone belts.  
77 The overall architecture of the terrane is dominated by N to NE-oriented lithodemic  
78 belts and shear zones. These are cross-cut by plutons of biotite-tonalite and  
79 metaluminous granitoids which generally form the cores of dome-like structures (Key  
80 et al., 2008). Migmatite gneiss has yielded a metamorphic age of around 2.97 Ga,  
81 while felsic metavolcanics from the terrane have yielded Nd  $T_{DM}$  ages ranging from  
82 3.05 to 3.60 Ga (Chardon, 1997) illustrating the contribution of older crustal source  
83 components (Key et al., 2008). Younger tectonothermal events are recorded by  
84 tonalitic intrusions dated using U-Pb geochronology at  $2933 \pm 16$  Ma along with a  
85 syntectonic augen granite from the Tâçarât-Inemmaûdene Shear Zone intervening  
86 between the Tasiast-Tijirit Terrane and adjacent Amsaga Complex, dated at  $2954 \pm 11$   
87 Ma (Key et al., 2008).

88

### 89 2.2. *Amsaga Complex*

90

91 The Amsaga Complex was first surveyed by Barrère (1967) who outlined a number of  
92 informal lithologic associations. Recent mapping (Pitfield et al., 2005; O’Connor et  
93 al., 2005) has confirmed that a large part of the complex comprises a diverse  
94 association of quartzo-feldspathic granoblastic and migmatitic gneisses of tonalitic,  
95 trondhjemitic and granodioritic composition as well as hypersthene-bearing  
96 charnockitic gneisses with minor units of garnet-cordierite-sillimanite gneiss and  
97 basic – ultrabasic rocks, interleaved along a network of arcuate NNE- to N-trending  
98 ductile shear zones. Much of the Amsaga Complex preserves steep proto- to  
99 ultramylonitic fabrics associated with the array of ductile shear zones that dissect the  
100 region. However, competent quartzofeldspathic gneisses locally preserve areas of  
101 relatively low-strain and exhibit consistent NE-SW striking subvertical planar fabrics

102 (O'Connor et al., 2005).

103 Formation of gneisses in the Amsaga Complex has been constrained by ages  
104 of around 3.50 and 3.40 Ga (Auvrey et al., 1992; Potrel, 1994; Potrel et al., 1996)  
105 including orthogneiss dated by the U-Pb method at  $3515 \pm 15$  Ma and  $3422 \pm 10$  Ma  
106 (Potrel et al., 1996). Incorporation of an even older crustal component is suggested by  
107 Nd  $T_{DM}$  ages of around 3.60 Ga (Potrel et al., 1996). A subsequent event has been  
108 proposed based on U-Pb dating of charnokite at  $2986 \pm 8$  Ma (Potrel et al., 1998). The  
109 youngest thermal/magmatic event preserved in the complex was proposed by Potrel et  
110 al. (1998) on the basis of a granulitic gabbro dated by Auvrey et al. (1992) at around  
111 2.71 Ga. This is supported by dating of discrete, apparently post-tectonic granite  
112 bodies including the Touijenjert Granite, which cross-cuts gneisses of both the  
113 Amsaga Complex and Tasiast-Tijirit Terrane and provides a minimum age for their  
114 amalgamation. This granite has yielded U-Pb ages of  $2715 \pm 11$  Ma and  $2726 \pm 7$  Ma  
115 (Auvrey et al., 1992; Potrel et al., 1998) and a Sm-Nd mineral isochron age for an  
116 associated gabbro of  $2705 \pm 54$  Ma (Potrel et al., 1998). Their petrogenesis involved  
117 recycling of older crustal source components indicated by Nd  $T_{DM}$  ages of around 3.2  
118 to 3.1 Ga (Potrel, 1994; Potrel et al., 1996; 1998).

119

### 120 2.3. *Tiris Complex*

121

122 The Amsaga Complex is juxtaposed against the Tiris Complex along a broad  
123 belt of aluminous gneisses (Bronner, 1977; Rocci et al., 1991; O'Connor et al., 2005).  
124 To the northeast, these pass into an extensive complex dominated by foliated and  
125 unfoliated granitic rock, locally hypersthene-bearing aluminous or migmatitic gneiss  
126 and ferruginous quartzite with several large (up to around 20 km long) bodies of  
127 amphibolite. The only published ages from the Tiris Complex are Rb-Sr isochron ages  
128 of  $2779 \pm 83$  Ma and  $2706 \pm 71$  Ma from granulite facies gneisses (Vachette & Bronner,  
129 1975; Vachette, pers comm., in Cahen et al., 1984). The geology of the complex is  
130 described in more detail below.

131 The Tiris Complex is locally tectonically intercalated with metasediments of the  
132 Ijil Complex. The most extensive outcrop of this unit forms Kediat Ijil (Fig. 3), a broad  
133 inselberg south of the town of Zouerate comprising metasediments including  
134 ferruginous quartzite, capped by a distinctive conglomerate unit. Previous workers have  
135 interpreted the Ijil Complex as a klippe of Palaeoproterozoic rocks, resting

136 allochthonously on Archaean basement of the Tiris Complex (e.g. Bronner, 1977;  
137 Bronner & Chauvel, 1979; Bronner et al., 1992; Huon et al., 1992, Schofield &  
138 Gillespie, 2007).

139

#### 140 2.4. *Ghallaman Complex*

141

142 Two lithostratigraphic associations are recognised within the Mesoarchaean  
143 basement of the Ghallaman Complex (Lahondère et al., 2003): the Temmimichate-  
144 Tsabaya Complex comprising a granulite facies, basic to ultrabasic, meta-igneous  
145 association, and the Zednes Suite (Fig. 2), an association of tonalitic plutonic and  
146 gneissose rocks dated at around  $3044 \pm 5$  Ma, intruded by a suite of unfoliated  
147 granite-granodiorites dated at  $2915 \pm 18$  and  $2832 \pm 4$  Ma (Lahondère et al. 2003).  
148 Relationships between the domain and the Tiris Complex are largely obscured by  
149 younger cover rocks and superficial deposits. However, recent surveying has  
150 demonstrated that gneisses of the Temmimichate-Tsabaya Complex are structurally  
151 contiguous with granitic gneisses and ferruginous quartzites of the Tiris Complex,  
152 have at least some penetrative deformation in common and share the same overall W-  
153 E structural grain dominant in that area (Schofield et al., 2003; O'Connor et al., 2005).

154

155

### 156 3. **Geology of the Tiris Complex**

157

158 In general, the Tiris Complex comprises a region of granitoid domes with  
159 intervening keels of supracrustal rocks, crosscut by linear belts of tight folding and steep  
160 fabrics. It is estimated to comprise approximately 70% granite (*sensu stricto*) and  
161 contrasts markedly with the adjacent Archaean units. The following provides a  
162 description of the granite lithologies, their host rocks and overall structural setting.

163

#### 164 3.1. *Lithodemic divisions*

165

166 The new geological survey of the region (O'Connor et al., 2005) has defined  
167 three units within the Tiris Complex that are as follows:

168

##### 169 3.1.1. *El Gheicha Formation*

170 The El Gheicha Formation crops out in the southwestern part of the study area  
171 (Fig. 3). It preserves an arcuate contact with the Mirikli Formation to the NW,  
172 following the overall structural grain of the region and is near-coincident with the  
173 southern limit of bands of ferruginous quartzite and northern limit of aluminous facies  
174 recognised by Bronner (1977). It typically preserves locally migmatitic, cordierite and  
175 biotite bearing gneisses with or without garnet, sillimanite or kyanite and more rarely  
176 orthopyroxene as well as thin, impersistent units of ferruginous rock and metamafite  
177 (see Supplementary Data A for lithological details). The garnet-cordierite-sillimanite  
178  $\pm$  spinel and orthopyroxene-bearing assemblages preserved in the El Gheicha  
179 Formation indicate granulite facies conditions. The gneisses are predominantly  
180 cordierite-bearing which indicates metamorphic conditions in the range 600-850°C  
181 and <8Kb. The southern margin of the unit is in contact with foliated porphyritic  
182 granite, with subordinate leucogranite and gabbro-norite of the F'Derik Suite, which  
183 intervenes between the Tiris and Amsaga complexes. This magmatic suite is confined  
184 within an anastomosing plexus of ductile shear zones that juxtapose these two units. It  
185 is elongate and foliated parallel to the shear zone and interpreted as being syn-  
186 tectonic.

187

### 188 3.1.2. *Mirikli Formation*

189 The Mirikli Formation occupies the central and northeastern parts of the Tiris  
190 Complex (Fig. 3) and comprises abundant schlieric granite, granite and monzonite (see  
191 Supplementary Data A for lithological details). These are locally foliated or migmatitic,  
192 preserving a variety of banded fabrics suggestive of both anatexis of source gneisses and  
193 cross-cutting, mixing and mingling of various intrusive facies. Grain scale and  
194 penetrative sub-solidus fabrics are also locally preserved within more homogeneous  
195 portions. Prominent bands of ferruginous quartzite and aluminous paragneiss are  
196 common throughout well-exposed parts of the unit; several of these are currently  
197 exploited as a source of iron ore. Bands and pods of metamafite (commonly  
198 amphibolite) are widespread. Calcsilicate-rock, aluminous gneiss, quartzite,  
199 quartzofeldspathic gneiss, hypersthene gneiss, 'charnockitic' granite and monzonite  
200 occur as minor lithological components. Widespread migmatitisation, the presence of  
201 mica (mainly biotite) in quartzofeldspathic rocks, and widespread occurrence of  
202 hornblende-bearing amphibolite indicates that large parts of the formation have not  
203 exceeded middle to upper Amphibolite Facies conditions. However, the presence of 2-

204 pyroxene-bearing metamafic rock at Guelb el Rhein and an occurrence of sillimanite-  
205 garnet-quartz-K-feldspar-plagioclase-cordierite gneiss at Guelb Touijinjert suggest that  
206 granulite facies assemblages are preserved locally in rocks of suitable (e.g. mafic or  
207 aluminous) composition. Cuney et al. (1975) reported granulite facies, peak  
208 metamorphic conditions from ferruginous quartzites containing quartz-orthopyroxene-  
209 magnetite  $\pm$  Ca-pyroxene  $\pm$  garnet assemblages.

210

### 211 3.1.3. *El Khadra Formation*

212 The El Khadra Formation is wholly enclosed by the Mirikli Formation and  
213 crops out in the north of the study area (Fig. 3). Like the Mirikli Formation, it consists  
214 of a lithologically variable assemblage of quartzofeldspathic and calc-silicate  
215 metasedimentary and (meta-) igneous rocks (see Supplementary Data A for  
216 lithological details). However, it is distinguished by a higher proportion of  
217 metasedimentary rock at outcrop and the common and widespread occurrence of  
218 numerous, generally closely-spaced bands of ferruginous quartzite. The dominantly  
219 quartzofeldspathic character of much of the formation is unhelpful in terms of  
220 determining metamorphic conditions. The metacarbonate rocks indicate the original  
221 limestones contained a range of impurities (silica, alumina etc.), rendering a precise  
222 estimation of metamorphic grade very difficult. Nevertheless, the widespread  
223 occurrence of metamafic rock in which amphibole is the principal mafic mineral  
224 suggests that the formation was metamorphosed under Amphibolite facies conditions.

225

226

### 227 3.2. *Structure*

228

229 Bronner (1992) indentified three domains in the Tiris Complex (Fig. 3) that  
230 provide a useful framework for description and interpretation of the structure. Despite  
231 marked contrasts between the three structural domains and intervening tectonic  
232 boundaries, contiguity of lithodemic units argues against an exotic relationship.

233 The structure of the southwestern part of the study area (SW domain) is  
234 characterised by NW-striking, steep to moderately inclined planar fabrics with  
235 steeply-plunging mineral lineations and NW-elongate, more or less upright elliptical  
236 folds (Fig 4a). At least three superposed fold generations are preserved in this domain  
237 with prominent type 3 interference figures (Ramsay, 1962) preserved at outcrop scale

238 (Fig. 5) indicating coplanar refolding of earlier inclined or recumbent structures. The  
239 last, upright fold generation (local F3) deforms a10's to 100's of metres-scale  
240 interlayering of metasedimentary units and foliated granitic rocks. The boundary  
241 between this structural unit and the Central Domain is taken at a steep, linear high  
242 strain zone extending NW from the southern margin of Kediat Ijil (Accident Sud  
243 Ijilien of Bronner, 1992; Fig. 3). This zone preserves increasing strain toward the NE  
244 margin of the domain in which folds become tighter, and locally isoclinal, fabrics are  
245 invariably steeply inclined and locally mylonitic with steeply plunging mineral  
246 lineations, locally cross-cut by narrow granitic dykes.

247 The central part of the Tiris Complex (Central domain) is characterised  
248 by the absence of a strong regional structural trend, although a history of  
249 polyphase folding is preserved within the thin units of metasedimentary rock  
250 (Bronner, 1992) that also attests to an early generation of recumbent  
251 structures and metamorphic fabrics. The overall structure is dominated by the  
252 "mantled gneiss domes" described by some earlier workers (e.g. Rocci et al.,  
253 1991). First order (local) F3 structures in this area form a series of impinging  
254 ellipsoidal, dome-shaped or sheath-like antiforms (Fig. 6), of several  
255 kilometres diameter, cored by foliated to unfoliated granite and migmatite, and  
256 separated by complex, tight synforms preserving the main units of ferruginous  
257 quartzite and metasedimentary gneiss. Hinges are strongly curvilinear and  
258 steeply plunging, and are associated with a well-developed, steeply, sub-  
259 radially plunging, mineral stretching lineation that is strongly developed in the  
260 metasediments, but largely absent from the granite cores (Fig. 4b). Granite  
261 fabrics are generally more intense toward the synformal margins of the  
262 domes, consistent with those in expanding or syn-kinematic plutons (e.g.  
263 Ramsay, 1981; Cruden, 1990) suggesting that they are coeval with  
264 dome/synform formation.

265 In the northeast of the study region (NE domain) the structure is characterised  
266 by an approximately W-trending grain and W-elongate, upright elliptical F3 folds.  
267 This domain is uniquely characterised by linear zones of steeply NE to SE-plunging  
268 *ls*-tectonites preserved in the metasedimentary rocks with local NE to SE-dipping  
269 planar fabrics (Fig. 4c). These are unaffected by earlier fold phases and are interpreted  
270 as recording the youngest deformation episode episode in this part of the study area.  
271 The northern margin of this domain is defined by the El M'dena Fault Zone (Fig. 2)



272 that juxtaposes the Ghallaman Complex against Late Archaean rocks and  
273 Palaeoproterozoic metasediments and granitoids intercalated during the ca. 2.1 Ga  
274 Eburnean Orogeny. The exposed southeastern margin of the domain is contiguous  
275 with another belt of imbricated metasedimentary rocks attributed to the Early  
276 Palaeoproterozoic Idjil Complex, the El M'haoudat range (Fig. 3).

277

278

279

280

#### 281 **4. U-Pb geochronology and Sm-Nd isotope geochemistry**

282

283 In order to augment the existing database of U-Pb analyses from the Reguibat  
284 Shield, four samples were collected from the Tiris Complex for geochronological  
285 study. The main aim was to constrain the age of the widespread granite magmatism  
286 preserved in this part of the shield to enable a more detailed understanding of its  
287 overall tectono-thermal evolution. The samples represent granites from the SW and  
288 Central structural domains, the Accident Sud Ijilien and the F'derik Suite. The NE  
289 structural domain was not represented, partly due to the dominance of  
290 metasedimentary rock and absence of suitable material for dating. U-Pb ages were  
291 determined by Laser Ablation Multi-Collector Inductively Coupled Plasma Mass  
292 Spectrometry (LA-MC-ICP-MS) at the NERC Isotope Geosciences Laboratory  
293 (NIGL), Keyworth, UK. Zircons were separated from the rock sample using standard  
294 separation techniques and mounted in 1" diameter epoxy resin mounts and polished  
295 down to expose an equatorial section through the crystals. Analyses were conducted  
296 following Thomas et al. (2009) except that GJ1 zircon was used as the primary  
297 reference material with 91500 and Plesovice run as validation materials. The  
298 Concordia age result for 91500 was  $1059.4 \pm 4.3$  Ma (weighted average Pb/U age =  
299  $1059.5 \pm 5.2$  Ma, MSWD = 1.3 n = 25) and the Concordia age result for Plesovice was  
300  $337.0 \pm 1.2$  Ma (weighted average Pb/U age =  $336.2 \pm 1.2$  Ma, MSWD = 0.57, n =  
301 49). Data were reduced and uncertainties propagated using an in-house spreadsheet  
302 calculation package with ages determined using the Isoplot 3.16 macro of Ludwig  
303 (2003). Despite careful selection of all mineral grains the zircons were of relatively  
304 poor quality resulting in largely discordant data. This is not unusual for zircons from  
305 Archaean and Proterozoic terranes and only interpretable, concordant data have been

306 plotted in the figures. All data are however provided in the supplementary data tables  
307 (Supplementary Data B).

308 Whole rock Sm-Nd isotope dilution analyses of the four samples used for U-  
309 Pb age determination were also carried out at NIGL using thermal ionisation mass  
310 spectrometry (ID-TIMS). Sample dissolution, chemical separation and analysis  
311 procedures are detailed in the supplementary text (Supplementary Data C). Tabulated  
312 results for both U-Pb and Sm-Nd analyses are lodged as supplementary materials  
313 (Supplementary Data D).

314

#### 315 4.1. *Sample 23120012*

316

317 This sample comprises pinkish-grey, biotitic, fine granite with scattered cm-  
318 scale biotitic clots and schlieren and was collected from the Mirikli Formation  
319 (23°02'49"N / 12°20'21"W). This sample was collected as a representative  
320 component of the syn-tectonic granite domes of the central structural domain with the  
321 aim of constraining the age of magmatism and dome formation, also providing a  
322 minimum age on the earlier flat lying structures. It yielded fairly poor quality zircons  
323 with no apparent cores or rims (Fig. 7a). Forty analyses were conducted on twenty  
324 seven zircons. Most of the analyses were strongly discordant; however, five near  
325 concordant analyses suggested two age components (Fig. 8a). These are interpreted to  
326 represent either crystallization of the granite at  $2948 \pm 11$  Ma with ancient Pb-loss or  
327  $2875 \pm 18$  Ma with inheritance. This sample yielded an  $^{67}\text{Nd}$  value of  $-1.4$  at  $t = 2948$   
328 Ma and  $T_{DM} 3.25$  Ga.

329

#### 330 4.2. *Sample 22120276*

331

332 This sample comprises pink to red, schlieric, foliated, fine to medium grained,  
333 garnet-bearing, biotite granite and was collected from the Mirikli Formation in the  
334 SW domain (22°22'10"N / 12°37'00"W). The schlieric character (prominent biotite-  
335 rich clots and trails) points to an anatectic origin. This sample was collected to  
336 provide a date for magmatism in this domain. Monazite (Fig. 7b) and variable quality  
337 zircons were recovered from the sample. The zircons were mainly elongate with some  
338 larger, more blade-like crystals (Fig. 7c). Eight monazites and fifteen zircons were  
339 analysed, multiple times in the case of zircon. Fifteen zircon analyses were included

340 in a Concordia age result (Fig. 8b) of  $2654 \pm 8$  Ma ( $2\sigma$ ). This is interpreted to  
341 represent the crystallisation age of the rock. Seven of the eight monazite analyses  
342 result in a concordia age of  $2482 \pm 7$  Ma ( $2\sigma$ , Fig. 8c). This is interpreted to represent  
343 the timing of metamorphism that crystallised the garnet in this sample. This sample  
344 yielded an  $^{67}\text{Nd}$  value of  $-1.9$  at  $t = 2654$  Ma and  $T_{DM} 3.04$  Ga.

345

#### 346 4.3. *Sample 22120262*

347

348 This sample was collected from the Mirikli Formation within the high strain  
349 zone of the Accident Sud Ijilien ( $22^{\circ}37'20''\text{N} / 12^{\circ}42'15''\text{W}$ ) and comprises foliated,  
350 weakly porphyroclastic, biotitic metagranitic rock sampled from one of a series of  
351 dyke-like intrusions forming 10 m-scale bodies cross-cutting the main foliation  
352 adjacent to the Accident sud Ijilien. These bodies are interpreted as syn-tectonic and  
353 were collected in order to constrain the maximum age of deformation within this  
354 zone, post-dating the formation of pervasive gneissosities within the host rock.  
355 Modally, the rock lies close to the monzogranite-granodiorite boundary, and  
356 plagioclase is partly altered to clinozoisite and epidote. Heavy mineral separation  
357 yielded abundant zircon. Two distinct populations were distinguished (Fig. 7d). More  
358 than 90% of the grains were variably cloudy and altered, elongate, smaller crystals  
359 with aspect ratio of 2:1-5:1. The second population comprised clearer, more glassy-  
360 looking crystals, suggesting a lower uranium concentration than the first population.  
361 Of twenty-seven zircon analyses from this second population six provided near  
362 concordant data. The age spread suggests crystallization of the granite at  $2487 \pm 8$  Ma  
363 ( $2\sigma$ , Fig. 8d) with inheritance at c.2550 and 2700 Ma (Fig. 8d). This sample yielded  
364 an  $^{67}\text{Nd}$  value of  $-5.7$  at  $t = 2487$  Ma and  $T_{DM} 3.14$  Ga.

365

#### 366 4.4. *Sample 211200139*

367

368 This sample comprises porphyritic granite collected from the F'Derik Suite at  
369 the southern margin of the complex ( $21^{\circ}31'47''\text{N} / 12^{\circ}52'19''\text{W}$ ). This unit of  
370 syntectonic granitic rocks was collected to provide an age constraint on movement  
371 along the shear zone intervening between the Amsaga and Tiris complexes. It yielded  
372 good quality titanite and allanite (Fig. 7e) and good quality bipyramidal and elongate  
373 zircons (Fig. 7f). Thirty one analyses from twenty two zircons were performed on this

374 sample. Four analyses were excluded from a calculation giving a Concordia age of  
375  $2472 \pm 6$  Ma ( $2\sigma$ , Fig. 8e). This is interpreted to represent the crystallization age of  
376 the rock. This sample yielded an  $^{87}\text{Nd}$  value of  $-2.1$  at  $t = 2472$  Ma and  $T_{DM} 2.9$  Ga.

377

378

## 379 **5. Discussion**

380

381 Taken together with their field relationships, the U-Pb and Sm-Nd analyses presented  
382 herein provide new constraints on the geological evolution of the Tiris Complex.  
383 Despite significant challenges presented by the paucity of modern geochronological  
384 determinations, we go on to discuss these in the context of the evolution of the  
385 Reguibat Shield and West African Craton as a whole.

386

### 387 *5.1 Geological development of the Tiris Complex*

388

389 The oldest rocks preserved in the Tiris Complex, pre-dating the main phase of  
390 granite magmatism at around 2.95 Ga, comprise metasedimentary ferruginous  
391 quartzite and aluminous and hypersthene-bearing paragneiss of the Mirikli Formation.  
392 These may be equivalent to similar assemblages preserved in the El Khadra and el  
393 Geicha formations. The presence of bands and pods of metamafite intercalated with  
394 the metasedimentary host indicate that there was also an early phase of mafic dyke  
395 emplacement, although the age of this also remains unconstrained.

396 Early tectonism, also pre-dating the main intrusive episode, is recorded by  
397 structures common to all three structural domains. The earliest of these (F1) are flat-  
398 lying, probably high grade metamorphic fabrics and recumbent folds. Indeed, Bronner  
399 (1992) argued that there are in fact only a small number of units of ferruginous quartzite  
400 that are repeated by tight to isoclinal folding and associated thrust imbrication during the  
401 early phase of deformation.

402 One sample from the Mirikli Formation (23120012) was intruded between  
403  $2948 \pm 11$  Ma and  $2875 \pm 18$  Ma. This sample records the maximum age constraint on  
404 intrusion of nested dome like structures and development of elliptical periclinal folds  
405 (F3). The  $T_{DM}$  of 3.25 Ga from this sample, together with an intimate association  
406 between granite *sensu stricto* and anatectic migmatite lithologies implies contribution  
407 of older crustal material as a source component. A minimum age constraint for this

408 magmatic episode is provided by the crystallisation age of  $2654 \pm 8$  Ma for granite  
409 from the Mirikli Formation (22120276) along with inheritance at  $2691 \pm 11$  Ma from  
410 granite within the Accident Sud Ijilien (22120262). This was also associated with  
411 recycling of older crustal components indicated by  $T_{DM}$  of 3.14 and 3.04 Ga  
412 respectively from these samples. In this context, the Rb-Sr ages of  $2779 \pm 83$  Ma and  
413  $2706 \pm 71$  Ma could represent either partial isotopic resetting of the gneisses, although  
414 both analyses are also within error of one of the end member magmatic events.  
415 Similarly, a U-Pb age of  $2821 \pm 45$  Ma, lying within the range of magmatic ages from  
416 the Tiris Complex, was recorded as an inherited component in zircon from a sample  
417 of Palaeoproterozoic migmatite of the adjacent Eburnean mobile belt (Schofield et al.,  
418 2006).

419 In a previous review of the district, Rocci et al. (1991) concluded that the  
420 diapirs formed by partial melting of silicic metasedimentary rock, which ascended  
421 through denser, less readily fused metasediments that in turn tended to sink through  
422 the ascending melt. We concur with this conclusion having observed a predominance  
423 steeply plunging mineral lineations, which provide evidence for constrictional strain  
424 resulting from strong vertical extension (analogous to the “vertical tectonics” of  
425 McGregor, 1951), as well as concentric planar granite fabrics within the domes, which  
426 present an arrangement of structures typical of many diaper-like plutons (e.g.  
427 Schwerdtner, 1990). Together, the widespread migmatisation, granite intrusion and  
428 formation of nested diapiric domes are speculatively considered to record local  
429 convective overturning of the lithosphere (cf. Collins et al., 1998).

430 The younger intrusions from the Tiris Complex include foliated syntectonic  
431 granite within the Accident Sud Ijilien dated at  $2487 \pm 8$  Ma (22120262). This is  
432 interpreted to provide a minimum age for the formation of penetrative fabrics in the  
433 host gneisses. Granite from the F’Derik Suite (21100139), located within the high  
434 strain zone abutting the Amsaga Complex, yielded an age of  $2472 \pm 6$  Ma. Together,  
435 these illustrate an episode of more spatially-focussed magmatism localised within  
436 the major transecting shear zones during earliest Palaeoproterozoic times. This  
437 tectonothermal event clearly also had a wider influence in the region indicated by a U-  
438 Pb metamorphic age of  $2482 \pm 7$  Ma on monazite from one sample (22120276). This  
439 later phase of magmatism also involved input from older source components,  
440 indicated by  $T_{DM}$  of 3.14 and 2.9 Ga for these samples.

441 The latest penetrative tectonism to affect the Archaean Domain of the  
442 Reguibat Shield occurred during the ca. 2.1 Ga Eburnean Orogeny. To the NE of the  
443 Tiris Complex, the main Palaeoproterozoic mobile belt records metamorphism,  
444 granite magmatism, sinistral transpression and translation of Early Palaeoproterozoic  
445 units, including those of the Kediat Ijil across the Archaean foreland of the Tiris  
446 Complex (Schofield et al., 2006; Schofield & Gillespie, 2007). Rejuvenation of the  
447 partitioned shear zones in the Tiris Complex as thrusts and back-thrusts was implicit  
448 in the model of Schofield & Gillespie (2007), however the detailed structural  
449 relationships are less clear. In the NE of the complex, the presence of later inclined  
450 zones of *ls*-tectonites is indicative of NE-SW oriented non-coaxial horizontal  
451 translation that is speculatively consistent with overprinting Eburnean transpression as  
452 preserved in the adjacent suture zone and outliers including El M'haoudat and Kediat  
453 Idjil (Schofield et al., 2006).

454

#### 455 *5.2 Implications for assembly of the Reguibat Shield*

456

457 The oldest known rocks exposed in the Reguibat Shield are approximately 3.51  
458 Ga orthogneisses preserved in the Amsaga Complex. These were interpreted as potential  
459 source components to the younger supracrustal rocks with which they are intercalated  
460 and have been argued to provide a maximum age for their deposition (Potrel et al.,  
461 1996). A minimum age constraint is given by Granulite Facies metamorphism,  
462 constrained by the age of charnockite intrusion at around 2.98 Ga (Potrel, 1994; Potrel et  
463 al., 1996). Granulite Facies mineral assemblages from the Amsaga Complex  
464 metasediments compare well with those of aluminous gneisses in the Tiris Complex and  
465 provide a compelling link between the two units. This comparison is strengthened by  
466 the recognition of early high grade metamorphism and isoclinal folding in the Tiris  
467 Complex (Bronner, 1992), pre-dating ca. 2.95 Ga granite dome formation, as well as  
468 development of ca 3.04 Ga high grade gneisses in the Ghallaman Complex. In the  
469 Tasiast-Tijirit Terrane, no direct dating of supracrustal rocks has been carried out,  
470 although a zircon evaporation age on migmatite gneiss of around 2.97 Ga as well as Nd  
471  $T_{DM}$  values ranging between 3.05 and 3.60 Ga from felsic metavolcanics (Chardon,  
472 1997) suggest formation of the volcano-sedimentary succession prior to around 3.00 Ga,  
473 comparable to that of the Amsaga Complex metasediments.

474 From these available data it is evident that parts of all successions were  
475 deposited after around 3.60 Ga and prior to around 2.98 Ga. Furthermore, the overlap in  
476 age and prevalence of mafic volcanic rocks and units of ferruginous quartzite,  
477 predominant many Palaeo- Mesoarchaeon sedimentary successions (see review of  
478 Trendall & Blockley, 2004) illustrate clear commonalities between the Archaean  
479 supracrustal rocks.

480 Key et al. (2008) interpreted the intrusion of a syntectonic granite at 2.95 Ga  
481 intervening between the Amsaga Complex and adjacent Tasiast-Tijirit Terrane as  
482 recording the maximum age of amalgamation of these two terranes into their current  
483 positions, while the minimum age is constrained by intrusion of the Touijenjert Granite,  
484 dated at around 2.72 Ga (Auvrey et al., 1992; Potrel et al., 1998).

485 The proposed maximum age for amalgamation was accompanied by an  
486 episode of more widespread, protracted magmatism recorded by intrusion of  
487 charnockitic rocks from the Amsaga Complex which have yielded ages of 2.98 to 2.95  
488 Ga, as well as intrusion of discrete tonalitic plutons within the Tasiast-Tijirit Terrane,  
489 one of which has been dated at around 2.93 Ga (Key et al., 2008), and granitic  
490 intrusion in the Ghallaman Complex dated at 2.91 and 2.83 Ga (Lahondère et al.  
491 2003). In the Tiris Complex, granitic rocks of this age (ca. 2.95 and 2.87 Ga) contrast  
492 with similar age rocks elsewhere in the Reguibat Shield in that they form part of a  
493 broad belt as opposed to isolated post-tectonic plutons or linear syn-tectonic intrusions  
494 of the other units.

495 Noearchaeon magmatism is recorded in the shield by ca. 2.71 Ga post-tectonic  
496 granites (and gabbro) of the Tasiast-Tijirit Terrane as well as 2.69 and 2.65 Ga granite  
497 magmatism and inheritance from the Tiris Complex.

498 The strongly localized nature of younger, ca. 2.56 and 2.48 Ga, syn-tectonic  
499 granite intrusions in the Tiris Complex is reflected in their emplacement into major  
500 shear zones. Magmatism of this age has not been identified elsewhere in the shield  
501 and is interpreted as reflecting structural reactivation within the zone of earlier crustal  
502 reworking. During the ca. 2.1 Ga Eburnean Orogeny, The Tiris Complex occupied the  
503 outboard margin of the shield, attested to by further reactivation as well as accretion  
504 of adjacent Palaeoproterozoic successions and arc-granitoids.

505

506 *5.3 Archaean Crustal Evolution in the West African Craton*

507

508           The two exposures of West African Craton; the Leo Shield in equatorial West  
509 Africa and the Reguibat Shield to the north both comprise western Achaean and  
510 eastern Eburnean domains. Similar ages for tectonic events and structures illustrate  
511 co-evolution of the craton during Palaeoproterozoic times. However, modern studies  
512 of the Archaean Domain of the Leo Shield are poorly represented in the literature (see  
513 review of Rocci et al., 1991). In general the Archaean, Kenema Man Domain of the  
514 Leo Shield comprises belts of greenstone successions interleaved with granitic rocks.  
515 Williams (1988) described a typical greenstone succession as comprising ‘isolated  
516 elongate outcrops of basaltic amphibolites, minor ultramafites, overlain by a  
517 sedimentary succession of greywackes, pelites and banded iron formation’, ‘engulfed  
518 by and infolded into a heterogeneous granitic migmatite complex’. Recognition of  
519 granulite facies assemblages in some supracrustal belts in contrast with amphibolite  
520 facies assemblages in others led some workers to propose two distinctive  
521 tectonothermal events (e.g. Camil, 1984; Macfarlane et al., 1981), an earlier Leonian  
522 event and a younger Liberian event, constrained by a number of Rb-Sr isochron ages  
523 between around 3.12 Ga and 2.65 Ga (e.g. Camill & Tempier, 1982; Camil et al.,  
524 1983; Hurley et al., 1971). However, Williams (1978) and Williams & Culver (1988)  
525 contended that these two events reflected a progressive continuum of tectonothermal  
526 processes. According to Cahen et al. (1984) the best constrained age is that provided  
527 by Beckinsale et al. (1981) who reported a Pb-Pb isochron age of  $2960 \pm 96$  Ma from  
528 a granitoid that also yielded an Rb-Sr isochron age of  $2753 \pm 30$  Ma interpreted as  
529 resetting of the Rb-Sr system and illustrating the two end member tectonothermal  
530 events. This latter piece of evidence provides the most compelling comparison  
531 between the Leo and Reguibat shields as it illustrates that the main tectonothermal  
532 events in both regions are approximately coeval. Furthermore, both comprise an older  
533 greenstone-sediment succession with mafic and ultramafic rocks, as well as units of  
534 banded iron formation, but are locally dominated by intrusive granitic rocks and  
535 migmatite.

536

## 537 **6. Summary**

538

539 The Tiris Complex makes up the northeastern-most tectono-stratigraphic unit of the  
540 Archaean Domain of the Reguibat Shield. It comprises a complex of granitic and  
541 migmatitic gneisses as well as metasedimentary units that can be subdivided into a



542 several lithodemic units named the El Geicha, Mirikli and El Khadra formations after  
543 O'Connor et al. (2005). Of these the El Geicha and El Khadra formations are  
544 dominated by paragneisses, with the southernmost El Geicha formation locally  
545 preserving garnet-cordierite-sillimanite and orthopyroxene-bearing assemblages. The  
546 Mirikli Formation is dominated by granitic rocks that are most extensive in the central  
547 structural domain, characterized by extensive domes with intervening complex  
548 synforms cored by paragneiss including thin units of ferruginous quartzite. New U-Pb  
549 dating and whole rock Sm-Nd isotopic analysis from four samples of granitic rocks  
550 has provided constraint on the evolution of the complex as a whole. The main phase  
551 of magmatism recorded by the granite domes is dated by one sample (23120012) at  
552 either  $2948 \pm 11$  Ma with ancient Pb-loss or  $2875 \pm 18$  Ma with inheritance.  
553 Subsequent, Neoarchaeon, magmatism is recorded at  $2654 \pm 8$  Ma (22120276) along  
554 with inheritance at  $2691 \pm 11$  Ma (22120262). Foliated granite intrusions, interpreted  
555 as syn-tectonic, record later movements on transecting shear zones at  $2487 \pm 8$  Ma  
556 (22120262) and  $2472 \pm 6$  Ma (21100139) along with a U-Pb metamorphic age of  
557  $2482 \pm 7$  Ma on monazite from one sample (22120276). All these magmatic episodes  
558 involved contribution of older continental crust indicated by Nd  $T_{DM}$  values ranging  
559 from 3.25 to 2.9 Ga, the latter yielded by the youngest dated granite.

560 Comparison with other units allows a tentative chronology for the Archaean  
561 and Early Palaeoproterozoic evolution of the West African Craton as a whole to be  
562 proposed. This comprises: 1) formation of Eoarchaeon crust, illustrated by various Nd  
563  $T_{DM}$  values as well as the metamorphic age of orthogneisses exposed in the Amsaga  
564 Complex dated at around 3.51 Ga; 2) formation of a Mesoarchaeon greenstone-  
565 sedimentary province across the craton along with subsequent intrusion of dispersal  
566 and high grade metamorphism prior to; 3) a main magmatic event recording  
567 reassembly of individual terranes, crustal reworking and intrusion of large volumes of  
568 granitic magmas constrained between around 2.98 and 2.83 Ga; 4) a subsequent  
569 Neoarchaeon magmatic episode between around 2.71 and 2.65 Ga, largely confined to  
570 intrusion post-tectonic plutons and isotopic overprinting; 5) intrusion of late  
571 Neoarchaeon to Early Palaeoproterozoic syn-tectonic intrusions within reactivated  
572 shear zones adjacent to the outboard margin of the craton; 6) accretion of outboard  
573 Eburnean successions and localized structural reactivation at around 2.1 Ga.

574  
575

576 **Acknowledgements**

577

578 The work described in this paper was undertaken in 2004 as part of the Government  
579 of Mauritania and World Bank-funded (IDA 3206MAU) “Projet de Renforcement  
580 Institutionnel du Secteur Minier” (PRISM). The authors would like to thank the  
581 PRISM director, M. Samory Ould Soueidatt, for all his support in country. We also  
582 wish to thank Roger Key and Stephen Daly for providing invaluable reviews of this  
583 and earlier versions of the manuscript. David Schofield, Peter Pitfield, Martin  
584 Gillespie and Eugene O’Connor publish with the permission of the Executive  
585 Director, British Geological Survey, Natural Environment Research Council.

586

587

588 **References**

589

590

591 Auvrey, B., Peucat, J.J., Potrel, A., Burd, J.P., Caruba, C., Dars, R., Lo, K., 1992.  
592 Données géochronologiques nouvelles sur l’Archéen de l’Amsaga (Dorsale Réguibat,  
593 Mauritanie). Comptes Rendus des Séances de L’Académie des Sciences, Paris, 315,  
594 63-70.

595

596 Barrère, J., 1967. Le groupe Précambrien entre Atar et Akjoujt (Amsaga). Etude du  
597 métamorphisme profond et de ses relations avec la migmatisations. Mémoires de  
598 Bureau de Recherches Géologiques et Minières, 42.

599

600 Beckinsale, R.D., Gale, N.H., Pankhurst, R.J., Macfarlane, A., Crow, M.J., Arthurs,  
601 J.W., Wilkinson, A.F. 1980. Discordant Rb-Sr and Pb-Pb whole rock isochron ages  
602 for the Archaean basement of Sierra Leone Precambrian Research, 13, 63-76.

603

604 Bessoles, B., 1977. Géologie de l’Afrique. Le craton Ouest Africain. Mémoires de  
605 Bureau de Recherches Géologiques et Minières, 88.

606

607 Bird, P., 1978. Initiation of intracontinental subduction in the Himalaya. Journal of  
608 Geophysical Research, 85, 4975-4987.

609

610 Bronner, G., 1977. Carte géologique de F'Dérik-oum Dférat à 1: 100,000. Marseille,  
611 Travaux des Laboratoires des Sciences de la Terre, 10.

612

613 Bronner, G., 1992. Structure et evolution d'un craton archéen. La dorsale Réguibat  
614 occidentale (Mauritanie). Tectonique et métallogénie des quartzites ferrugineux.  
615 Document du Bureau de Recherches Géologiques et Minières, 201.

616

617 Bronner, G., Chauvel, J.J., 1979. Precambrian ferruginous quartzites of the Ijil group  
618 (Kediat Ijil, Reguibat Shield, Mauritania). *Economic Geology*, 74, 77-94.

619

620 Bronner, G., Chauvel, J.J., Triboulet, C., 1992. Les formations ferrifères du  
621 Précambrien du Mauritanie: origine et evolution des quartzites ferrugineux.  
622 *Chronique de la Recherche Minière*, 508, 3-27.

623

624 Cahen, L., Snelling, N. J., Delhal, J., Vail, J.R., 1984. *The Geochronology and*  
625 *Evolution of Africa*. Clarendon Press, Oxford.

626

627 Camil, J. 1984. *Pétrographie, chronologie des ensembles granulitiques archéens et*  
628 *formations associées de la region de Man (Côte d'Ivoire). Implications pour l'histoire*  
629 *géologique du craton oust-africain. Thèse Université Adibjan, Côte d'Ivoire, 79.*

630

631 Camil, J., Tempier, P. 1984. Age à 2850 Ma determine par la method Rb-Sr sur roche  
632 totale pour la série des gneiss à hypersthene et granulites roses associées dans la  
633 region de Man (Côte d'Ivoire). Signification de l'âge archéen. *Comptes Rendus des*  
634 *Séances de L'Académie des Sciences, Paris, 294, 131-133.*

635

636 Camil, J., Tempier, P., Caen-Vachette, M. 1983. Schéma chronologique et structural  
637 des formations de la région de Man (Côte d'Ivoire). *12<sup>th</sup> Colloquium of African*  
638 *Geology (abstract), p. 18.*

639

640 Chardon, D., 1997. Les deformations continentals Archéennes. Exemples naturels et  
641 modélisation thermomécanique. *Mémoires de Géosciences, Rennes, 76.*

642

643 Collins, W.J., Van Kranendonk, M.J., Teyssier, C., 1998. Partial convective overturn  
644 of Archaean crust in the east Pilbara craton, western Australia: driving mechanisms  
645 and tectonic implications. *Journal of Structural Geology*, 20, 1405-1424.

646

647 Cruden, A.R., 1990. Flow and fabric development during the diapiric rise of magma.  
648 *Journal of Geology*. 98, 681 - 698.

649

650 Cuney, M., Bronner, G., Barbey, P., 1975. les paragenèses catazonales des quartzites  
651 à magnetite de la province ferrifère du Tiris (Précambrien de la dorsale Reguibat,  
652 Mauritanie). *Pétrologie*, 1, 103-120.

653

654 Dillon, W.P., Sougy, J M.A., 1974. Geology of West Africa and Cape Verde Islands,  
655 in: Nairn A. E. M., Stehl, F. G. (Eds.) *The ocean basins and margins*, Vol. 2, The  
656 North Atlantic, Plenum, London, pp. 315-390.

657

658 Huon, S., Bronner, G., Vauchez, A., 1992. Le Groupe allochtone d'Ijil (dorsale  
659 Reguibat, Mauritanie): témoin d'une chaîne intracratonique du Protérozoïque  
660 inférieur. 14<sup>ème</sup> Réunion Annuelle des Sciences de la Terre, Résumé, 80.

661

662 Huppert, H.E., Sparks, R.S.J., 1988. The generation of granitic magmas by intrusion  
663 of basalt into continental crust. *Journal of Petrology*, 29, 599-624.

664

665 Hurley, P.M., Leo, G.W., White, R.N., Fairbairn, H.W. 1971. Liberian age province  
666 (about 2700 Ma) and adjacent provinces in Liberia and Sierra Leone. *Geological*  
667 *Society of America, Bulletin*, 82, 3483-3490.

668

669 Isley, A.E., Abbott, D.H. 1999. Plume-related mafic volcanism and the deposition of  
670 banded iron formation. *Journal of Geophysical Research, B, Solid Earth and Planets*,  
671 104, 15,461-15,477.

672

673 Key, R.M., Loughlin, S.C., Horstwood, M.S.A., Gillespie, M., Pitfield, P.E.J.,  
674 Henney, P.J., Crowley, Q.G., Del Rio, M., 2008. Two Mesoarchaean terranes in the

675 Reguibat shield of NW Mauritania, in: Ennih, N., Liégeois, J-P. (Eds.), Boundaries of  
676 the West African Craton. Special Publication of the Geological Society, London, 297,  
677 pp. 33-52.

678

679 Lahondère, D., Thiéblemont, D., Goujou, J-C., Roger, J., Moussine-Pouchkine, A., Le  
680 Métour, J., Cocherie, A., Guerrot, C., 2003. Notice explicative des cartes géologiques  
681 et gîtologiques à 1/200 000 et 1/500 000 du Nord de la Mauritanie. Volume 1. DMG.  
682 Ministère des Mines et de l'Industrie, Nouakchott.

683

684 Ludwig, K.R., 2003. Isoplot 3, A Geochronological toolkit for Microsoft Excel.  
685 Berkeley Geochronology Centre Special Publication 1a.

686

687 Macfarlane, A., Crow, M.J., Arthur, J.W., Wilkinson, A.F., Alcott, J.W. 1981. The  
688 geology and mineral resources of northern Sierra Leone. Overseas Memoir, Institute  
689 of Geological Sciences, No. 7.

690

691 McGregor, A. M., 1951. Some milestones in the Precambrian of Southern Rhodesia.  
692 Transactions of the Geological Society of Africa, 54, 27-71.

693

694 O'Connor E.A., Pitfield, P.E.J., Schofield, D.I., Coats, S., Waters, C., Powell, J.,  
695 Ford, J., Clarke, S., Gillespie, M., 2005. Notice explicative des cartes géologiques et  
696 gîtologiques à 1/200 000 et 1/500 000 du Nord-Ouest de la Mauritanie. DMG,  
697 Ministère des Mines et de l'Industrie, Nouakchott.

698

699 Pitfield, P. E. J., Key, R. M., Waters, C. N., Hawkins, M. P. H., Schofield, D. I.,  
700 Loughlin, S., Barnes, R. P., 2005. Notice explicative des cartes géologiques et  
701 gîtologiques à 1/200 000 et 1/500 000 du Sud de la Mauritanie. Volume 1 –géologie.  
702 DMG, Ministère des Mines et de l'Industrie, Nouakchott.

703

704 Potrel, A., 1994. Evolution tectono-métamorphique d'un segment de croûte  
705 continentale archéene. Exemple de l'Amsaga (R.I. Mauritanie), Dorsale Réguibat  
706 (Craton ouest africain). Mémoire Géosciences Rennes, 56.

707

708 Potrel, A., Peucat, J.J., Fanning, C.M., Auvrey, B.M., Burg, J.P., Caruba, C., 1996.  
709 3.5 Ga old terranes in the West African Craton, Mauritania. *Journal of the Geological*  
710 *Society, London*, 153, 507-510.  
711  
712 Potrel, A., Peucat, J.J., Fanning, C.M., 1998. Archaean crustal evolution of the West  
713 African Craton: example of the Amsaga Area (Reguibat Rise). U-Pb and Sm-Nd  
714 evidence for crustal growth and recycling. *Precambrian Research*, 90, 107-117.  
715  
716 Ramsay, J.G., 1962. Interference patterns produced by the superposition of folds of  
717 similar types. *Journal of Geology*, 70, 466-481.  
718  
719 Ramsay, J.G., 1981. Emplacement mechanics of the Chindamava batholith,  
720 Zimbabwe. *Journal of Structural Geology*, 3, 93.  
721  
722 Rocci, G., Bronner, G., Deschamps, M., 1991. Crystalline Basement of the West  
723 African Craton, in: Dallmeyer R D., L  corch  , J P. (Eds.) *The West African Orogens*  
724 *and Circum-Atlantic Correlatives*, Springer Verlag, Berlin, pp. 31-61.  
725  
726 Schwerdtner, W.M., 1990. Structural tests of diapir hypotheses in Archaean crust of  
727 Ontario. *Canadian Journal of Earth Sciences*, 27, 387-402.  
728  
729 Schofield, D.I., Pitfield, P.E.J., Jordan, C.J., Wildman, G. & Bateson, L. 2003. Carte  
730 Geologique de la r  gion Oussat-Sfariat (Nord Mauritanie)    1:200 000. OMRG,  
731 Minist  re des Mines et de l'Industrie, Nouakchott.  
732  
733 Schofield, D. I., Gillespie M. R. 2007. A tectonic interpretation of "Eburnean  
734 terrane" outliers in the Reguibat Shield, Mauritania. *Journal of African Earth*  
735 *Sciences*, 49, 179-186.  
736  
737 Schofield, D.I., Horstwood, M.S.A., Pitfield, P.E.J., Crowley, Q.G., Wilkinson, A.F.,  
738 Sidaty, H.C.O., 2006. Timing and kinematics of Eburnean tectonics in the central  
739 Reguibat Shield, Mauritania. *Journal of the Geological Society, London*, 163, 549-  
740 560.  
741

742 Thomas, R.J., De Waele, B., Schofield, D.I., Goodenough, K.M., Horstwood, M.,  
743 Tucker, R.D., Bauer, W., Annells, R.A., Howard, K., B., Walsh, G., Rabarimanana,  
744 M., Rafahatelo, J.M., Ralison, A.V., Randriamananjara, T., 2009. Geological  
745 Evolution of the Neoproterozoic Bemarivo Belt, northern Madagascar. *Precambrian*  
746 *Research*, 172, 279-300.

747

748 Trendall, A.F., Blockley, J.G. 2004. Precambrian Iron-formation, in: Erickson, P.G.,  
749 Altermann, W., Nelson, D.R., Mueller, W.U., Catuneanu, O. (Eds) *The Precambrian*  
750 *Earth: Tempos and Events*, pp. 403-420.

751

752 Vachette, M., Bronner, G., 1975. Ages radiométriques Rb/Sr de 2.900 et 2.700 m.a.  
753 des series précambriennes de l'Amsaga et du Tiris, Dorsale Réguibat (Mauritanie).  
754 *Travaux des Laboratoires des Sciences de la Terre*, 11, 147-148.

755

756 Williams, H.R. 1978. The Archaean geology of Sierra Leone. *Precambrian Research*,  
757 6, 251-268.

758

759 Williams, H.R., 1988. The Archaean Kasila Group of Western Sierra Leone : Geology  
760 and relations with adjacent granite-greenstone terrane. *Precambrian Research*, 38,  
761 201-213.

762

763 Williams, H.R., Culver, S.J. 1988. Structural terranes and their relationships in Sierra  
764 Leone. *Journal of African Earth Sciences*, 7, 473-477.

765

766

767

768

769 **Figure 1.** Regional geology of West Africa.

770

771 **Figure 2.** Geological sketch map of the Archaean domain of the Reguibat Shield.

772 MF: El M'dena Fault. Box indicates approximate area of detailed survey.

773 \*Temmimchate-Tsabaya Complex.

774

775 **Figure 3.** Geological sketch map of the BGS 1: 200 000 scale survey area. A:  
776 area of Fig. 5; B: area of Fig. 6; KI: Kediat Ijil; M: El M'haoudat range; AI: Accident  
777 Sud Ijilien. Ages are U-Pb zircon or monazite (mon) reported herein. NE, Central and  
778 SW domains after Bronner (1992).

779

780 **Figure 4.** Stereographic projections (equal area, lower hemisphere) representing  
781 planar and linear fabric elements from the Tiris Complex: a). SW Domain b); Central  
782 Domain; c). NE Domain. Circle: pole to planar fabric, square: direction and plunge of  
783 linear fabric.

784 **Figure 5.** Sketch map of the fold interference pattern outlined by ferruginous  
785 quartzite units in the SW structural domain in the area east of Gleib El Freidi, to the  
786 south of Kediat d'Ijil, derived largely from interpretation of satellite imagery and  
787 showing superpositioning of F3 over F2 isoclinal folds.

788 **Figure 6.** Sketch map of the Guelb el Aouj area in the Central structural domain,  
789 derived largely from interpretation of satellite imagery and incorporating some  
790 structural data from Bronner (1977) illustrating domical F3 structure with intervening  
791 tight synclines.

792

793 **Figure 7.** Photomicrographs of: a) zircons separated from sample 23120012; b)  
794 monazites analysed from sample 22120276; c) zircons analysed from sample  
795 22120276; d) populations of cloudy, altered zircons (Population 1; left) and glassy,  
796 clear zircons (Population 2; right) separated from sample 22120262; e) titanite (left)  
797 and allanite (right) separated from sample 211200139; f) zircons separated from  
798 sample 211200139.

799

800 **Figure 8.** U-Pb Concordia plots of: a) zircon analyses from sample 23120012; b)  
801 zircon analyses from sample 22120276; c) monazite analyses from sample 22120276;  
802 d) analyses of the second population of zircons from sample 22120276; e) Zircon  
803 analyses from sample 221200139.

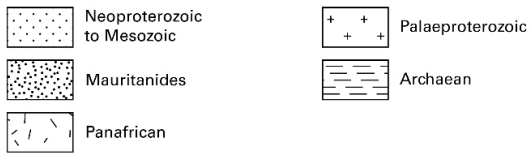
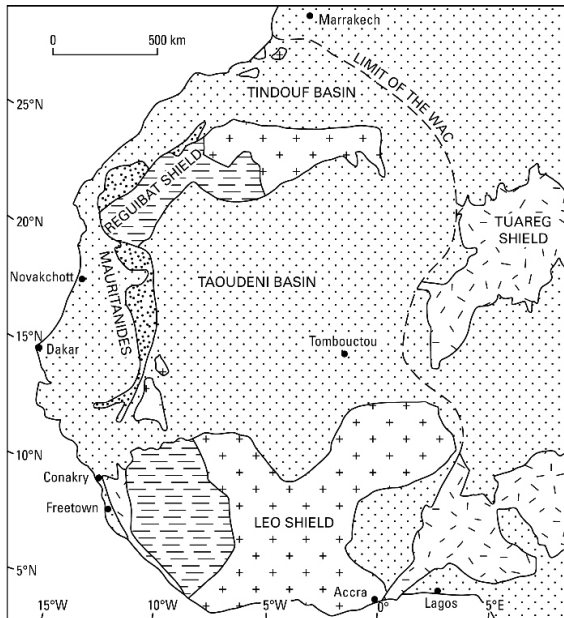
804

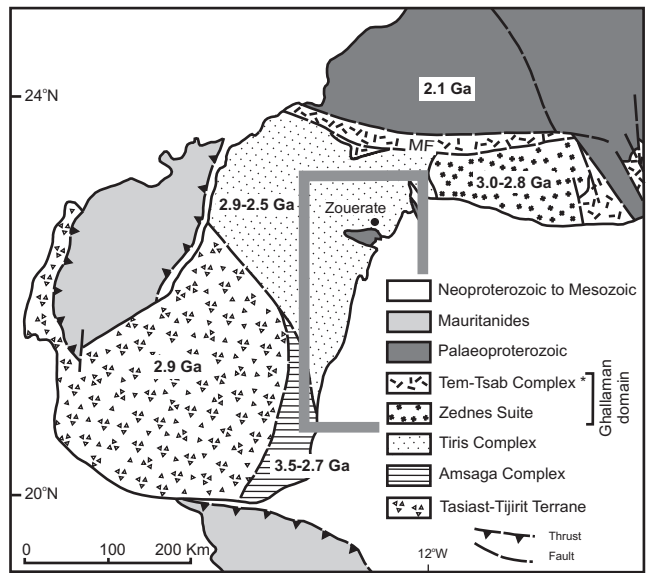
805

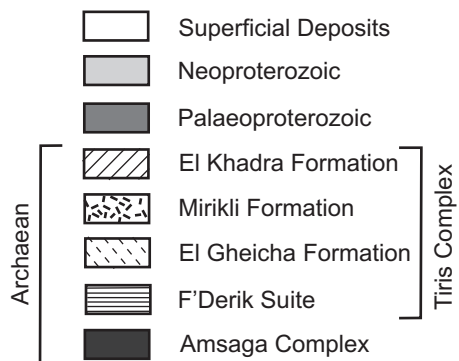
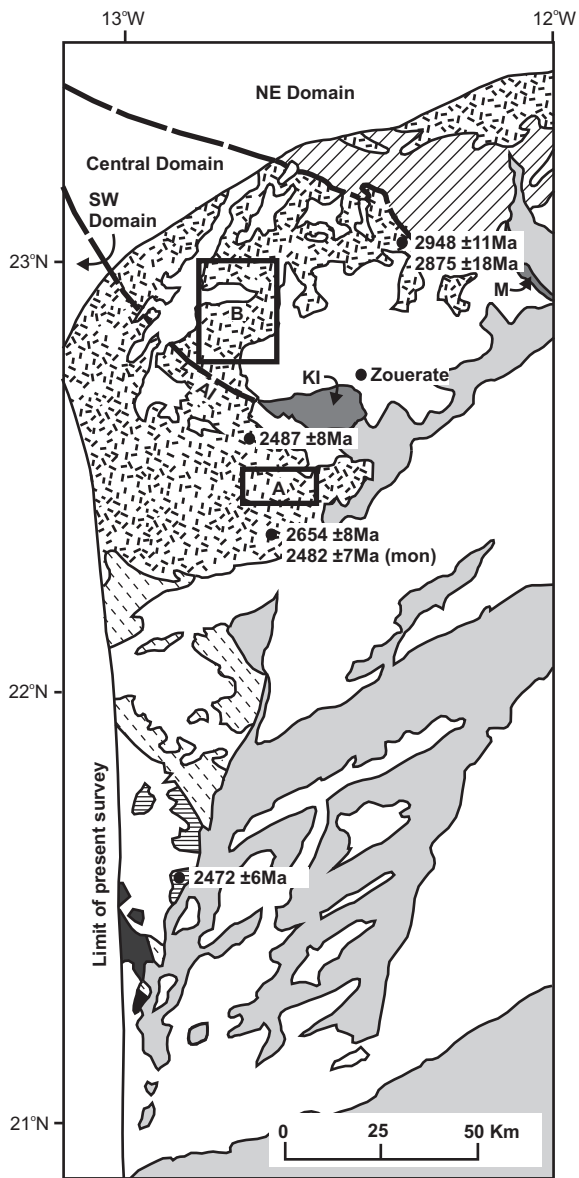
806

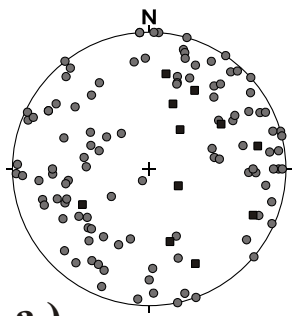
807



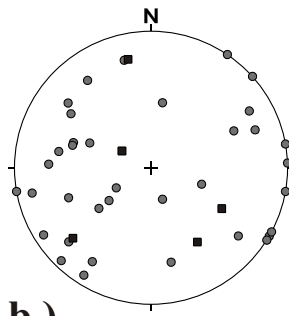




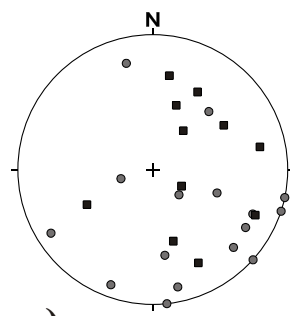




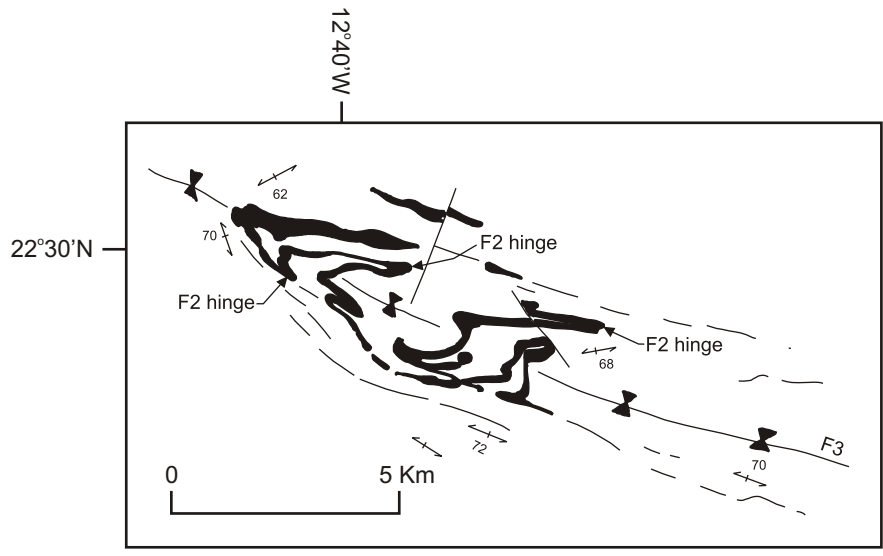
**a.)**

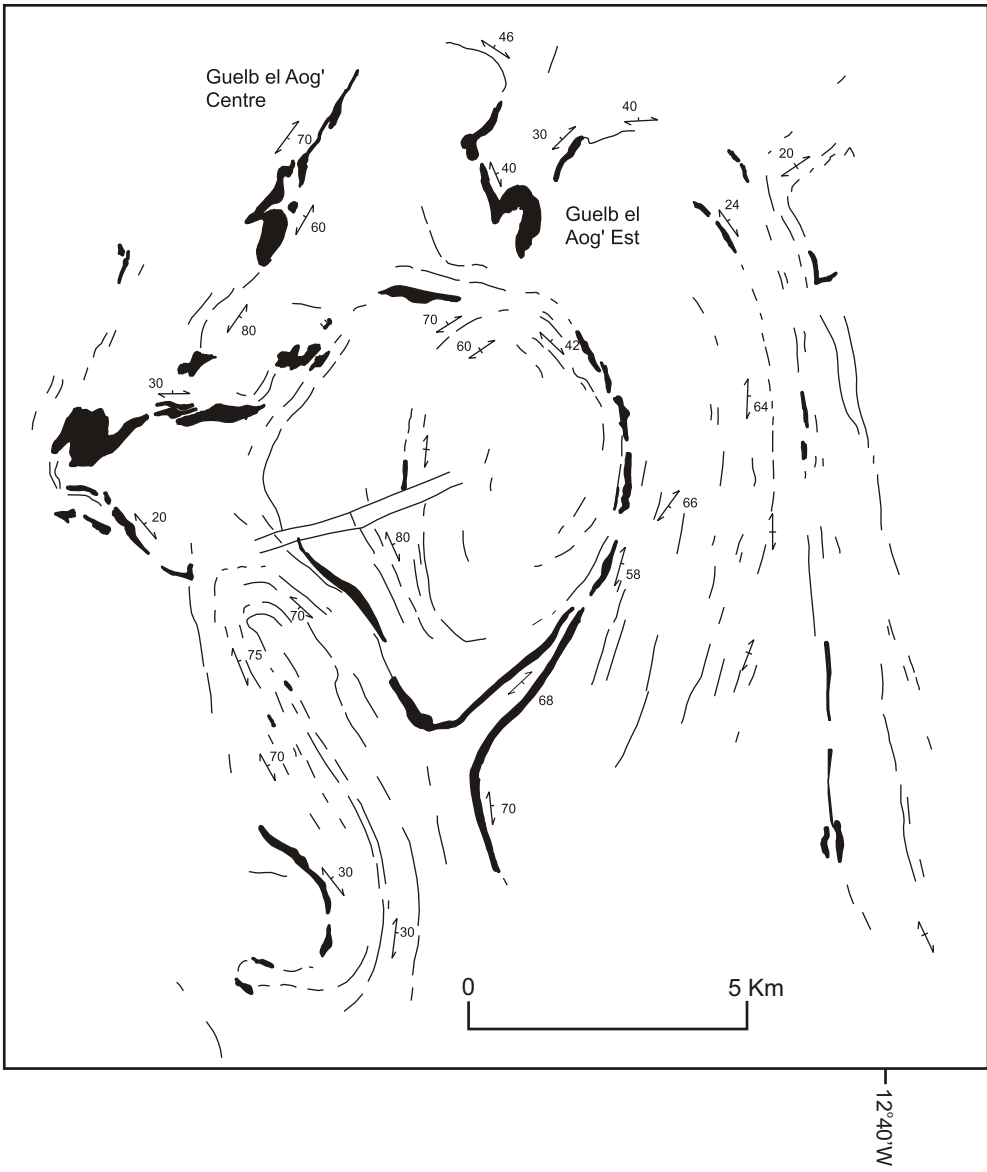


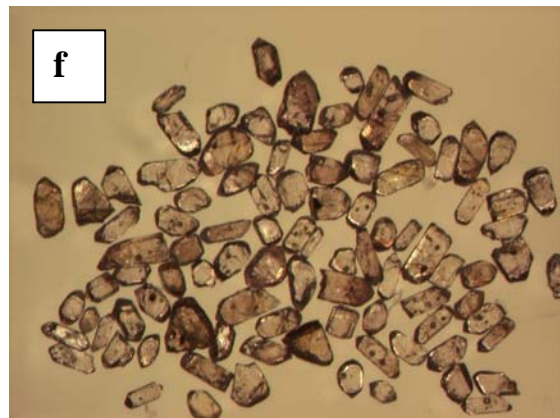
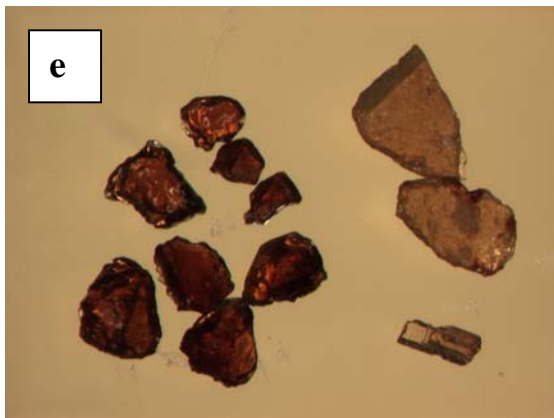
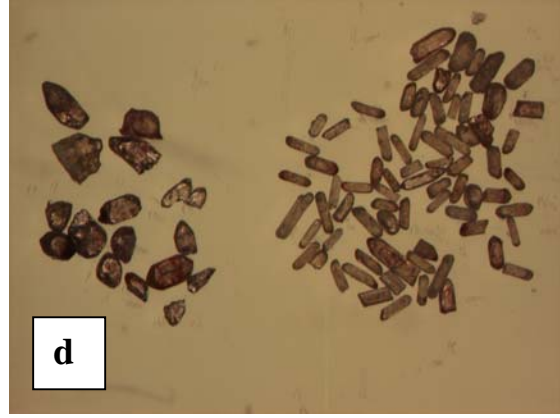
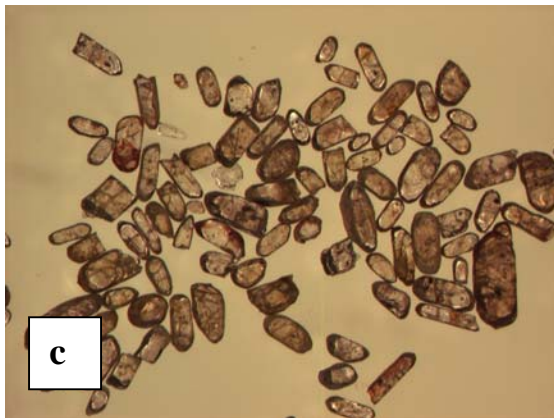
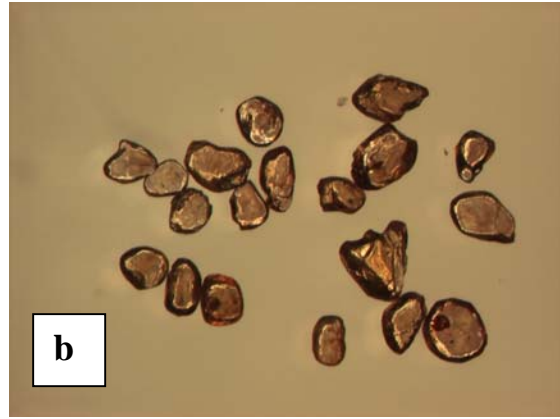
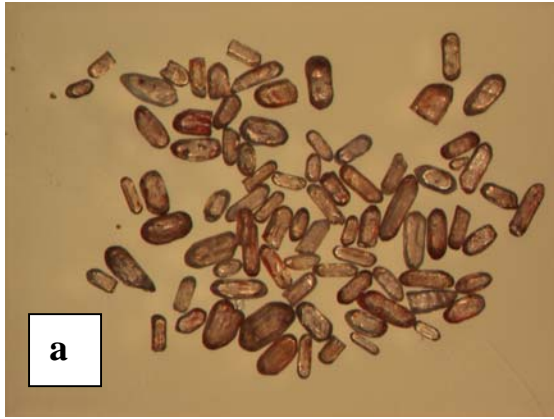
**b.)**



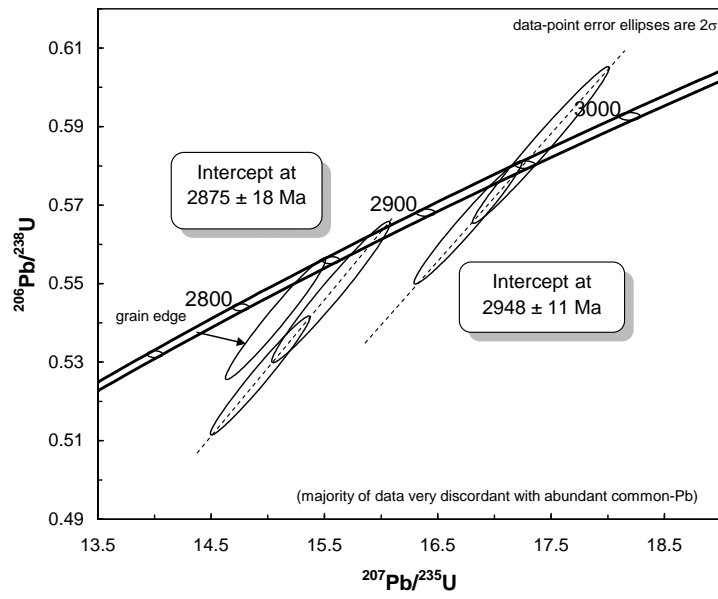
**c.)**



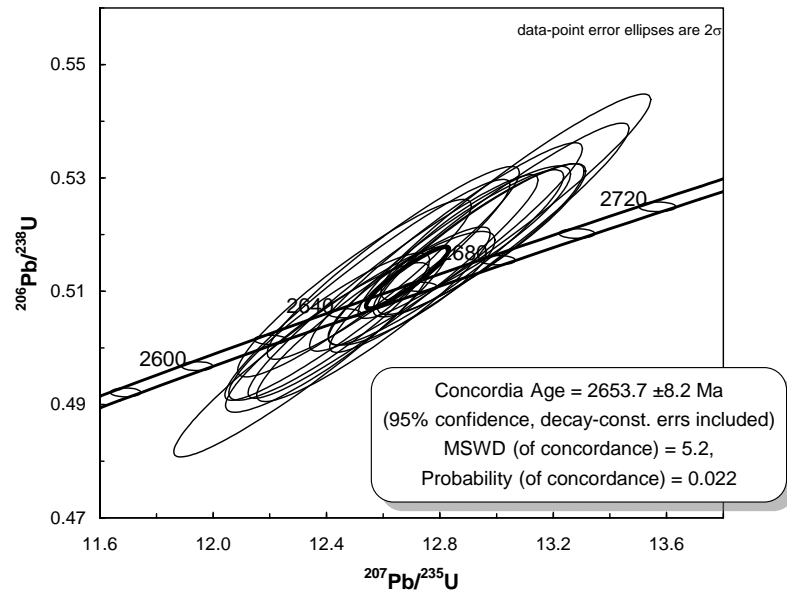




(a) 23120012

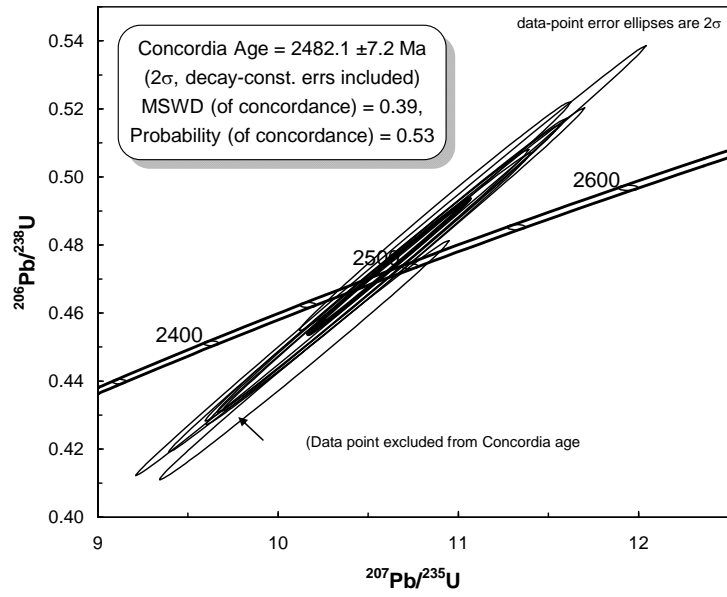


(b) 22120276 (zircon)

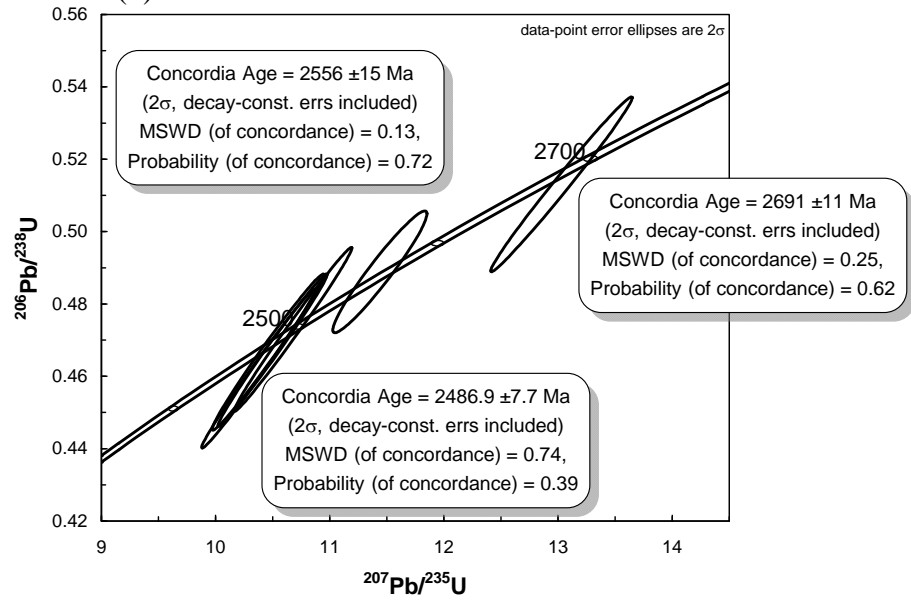




(c) 22120276 (monazite)



(d) 22120276



(e) 221200139

